BIOCELL
2023 47(7): 1583-1594

Tech Science Press

Ginsenoside Rg1 protects against ischemia-induced neuron damage by regulating the rno-miRNA-27a-3p/PPARγ axis

Yue GUAN[1,#]; Tingting ZHANG[2,#]; Jianan YU[3]; Jiawei LIU[4]; Wenyuan LI[5]; Yujia ZHENG[6]; Jiale WANG[3]; Yue LIU[3]; Fengguo ZHAI[2,7,*]

[1] Department of Clinical Medicine, Heilongjiang Nursing College, Harbin, 150001, China
[2] Department of Neurology, Hongqi Hospital of Mudanjiang Medical University, Mudanjiang, 157011, China
[3] Department of Pharmacology, Mudanjiang Medical University, Mudanjiang, 157011, China
[4] Department of Organic Chemistry, Mudanjiang Medical University, Mudanjiang, 157011, China
[5] Department of Anatomy, Mudanjiang Medical University, Mudanjiang, 157011, China
[6] Department of Rehabilitation Science, Kobe University Graduate School of Health Sciences, Kobe, 654-0142, Japan
[7] Institute of Natural Medicine, Mudanjiang Medical University, Mudanjiang, 157011, China

Key words: Ginsenoside Rg1, rno-miRNA-27a-3p, PPARγ, Cerebral ischemia, Neuron, OGD

Abstract: Background: A preliminary miRNA screening showed that expression levels of rno-miRNA-27a-3p were significantly increased in the serum and brain tissues of rats undergoing cerebral ischemia. In recent years, there is evidence of the protective capacity of the saponins extracted from panax ginseng and its primary active ingredient ginsenosideRg1oncerebral ischemic injury. **Methods:** Fetal rat neurons (FRNs) were cultured in glucose-and-serum-free medium and exposed to hypoxia to establish a cerebral ischemia model *in vitro* (oxygen and glucose deprivation model, OGD). Antioxidant indexes (CAT, SOD), inflammatory markers (MPO, TNF-α and IL-6), and the expression of apoptosis and proliferation associated proteins (NF kB-p65, Caspase 3-cleaved, BCL-2) were examined. **Results:** Pre-treatment of Rg1 (30–100 μg/mL) could effectively inhibit the decline of antioxidant indexes (CAT, SOD) and increase in inflammatory markers (MPO, TNF-α and IL-6), and effectively inhibited the apoptosis in FRNs induced by OGD in a gradient-dependent manner. The mechanism analysis showed that the role of Rg1 in protecting against ischemia-induced neuron damage depends on its indirect up-regulation of PPAR protein via suppression of rno-miRNA-27a-3p. Moreover, these effects of Rg1 could be reversed by exogenous rno-miRNA-27a-3p and PPAR gene silencing in FRNs exposed to OGD. **Conclusion:** To summarize, our study demonstrates that Rg1 could effectively attenuate neuronal damage caused by cerebral ischemia via the rno-miRNA-27a-3p/PPARγ pathway. Further, clarification of the novel mechanism will certainly improve our previous understanding of the role of Rg1 and enhancing its level in treatments for alleviating ischemic brain injury.

Introduction

Ischemic cerebrovascular diseases (ICVD) occur when blood flow to the brain is decreased or interrupted. ICVDs are characterized by high morbidity, mortality, and disability rates (Jian *et al.*, 2019). Currently, treatments for ICVD include thrombolytic therapy and neuroprotectant usage. However, thrombolytic therapy cannot be widely used in clinical practice due to narrow treatment time windows and complications from excessive bleeding while neuroprotectants are currently in the experimental stage. Thus, there remains an urgent need to find effective and safe therapies for ICVDs.

Panax quinquefolium (American ginseng) saponins (PQS) extracted from the stem and leaves of the plant have exhibited a variety of pharmacological functions such as anti-ischemia functioning, anti-arrhythmia roles, blood pressure reduction, blood sugar reduction, arteriosclerosis prevention (Wang *et al.*, 2006; Li *et al.*, 2017a; Wang *et al.*, 2007). Some studies have found that PQS could inhibit apoptosis activated by the endoplasmic reticulum apoptosis pathway, and reduce myocardial cell damage by reducing the expression of glucose regulatory protein 78 (GRP78),

*Address correspondence to: Fengguo Zhai, yxyzfg525@163.com
#These authors have contributed equally to this work
Received: 26 November 2022; Accepted: 20 March 2023;
Published: 23 June 2023

Doi: 10.32604/biocell.2023.028016

calreticulin (CRT), C/EBP-homologous protein (CHOP), caspase-12 and the pro-apoptotic protein Bax. Further, the expression of the anti-apoptotic protein Bcl-2 was shown to increase through pathological experiments such as ischemia/reperfusion (IR) and myocardial infarction (AMI) (Wang *et al.*, 2012a; Liu *et al.*, 2013). For many years, the study of the activity of traditional Chinese medicine has always been on the frontier and the hotspot of natural medicine research, and the effective pharmacological aspects of many traditional Chinese medicines have been deeply studied. Research data have confirmed that the Xinyue capsule has the effect of tonifying Qi and Yin, harmonizing blood, and protecting the heart, and is widely used in the treatment of coronary heart disease, with a definite and significant effect. Further, it can significantly relieve clinical symptoms and improve prognosis when used in the treatment of coronary heart disease. Basic research shows that the Xinyue capsule could intervene in coronary heart disease through multiple targets and multiple pathways (Liu, 2014). Given the similar pathological basis of ischemic diseases, researchers and medical workers are full of expectations and remain optimistic about the application of PQS in the treatment of cerebral ischemia.

Our group previously reported that PQS could protect against cerebral ischemia by increasing lactic dehydrogenase (LDH) and superoxide dismutase (SOD) activities, decreasing malondialdehyde (MDA) content, inhibiting the expression of apoptotic protein caspase-3, and elevating the expression of anti-apoptotic B-cell Lymphoma-2 (BCL-2) protein (Guan, 2008; Li *et al.*, 2010; Zhai *et al.*, 2011). The main components of PQS are saponins, amino acids, sugars, volatile oils, inorganic elements, and fatty acids (Ahuja *et al.*, 2018), of which saponins are the most important components. According to the structure of aglycone, saponins can be divided into oleanolic acid type, protopanaxadiol type and protopanaxatriol type (Feng *et al.*, 2017). The protopanaxadiol type mainly includes Rb1, Rb2, Rb3, Rc, Rd, Rg3 and Rh2; The original ginsenosides mainly include Re, Rf, Rg1, Rg2, Rh1, F1, F3, notoginsenoside R1, and oleanolic acids, which are Ro. Among them, Rb1, Re, Rd, Rg1, and Rb3 are considered to be the six main saponins, accounting for more than 70% of the total ginsenoside content in American ginseng (Shi *et al.*, 2019). Consistent and deep analysis of the effective and active ingredients of natural medicinal plants is the basic requirement of modern pharmaceutical research for identifying new drug targets and pathways.

As one of the active components of PQS, the efficacy of ginsenoside Rg1 has been demonstrated in ischemic stroke prevention and treatment by recent studies (Li *et al.*, 2017c; Yang *et al.*, 2015; Zhou *et al.*, 2014). Further, it was reported that ginsenoside Rg1 has protective effects on hypoxic-ischemic brain injury and neuronal apoptosis in rats (Zhang *et al.*, 2021). Some studies also found that ginsenoside Rg1 could inhibit the mitogen-activated protein kinase/nuclear transcription factor kappa B (MAPK/NF-κB) signal pathway and reduce the volume of cerebral infarction in rats with cerebral ischemia injury (Rong *et al.*, 2020). However, the mechanism of how Rg1 improves ischemia-induced injury remains unclear.

Using miRNA chip technology and real-time polymerase chain reaction (PCR), we previously identified 36 differentially expressed miRNAs in a rat model of cerebral ischemia, among which rno-miRNA-27a-3p expression was upregulated by 4.56 fold (Zhai *et al.*, 2012; Zhang *et al.*, 2012). The candidate targets of rno-miRNA-27a-3p were obtained using miRGen and predicted by three different prediction platforms (PicTar, Target Scan, and miRanda). The results were subsequently analyzed by Gene Ontology (GO) analysis. We found that PPARγ was one of the predicted targets of rno-miRNA-27a-3p. We hypothesized that rno-miRNA-27a-3p may regulate PPARγ which is involved in inflammation, oxidative stress, apoptosis, and the development of ICVD. In this study, we established an oxygen and glucose deprivation (OGD) model of rat embryonic neurons *in vitro* which was used to verify the anti-ischemic effect of Rg1 and clarify whether its mechanism is related to the rno-miRNA-27a-3p/PPARγ axis. The confirmation of the mechanism and effects of Rg1 on ischemic injury should offer novel insights into future implications for the therapeutic development of ICVD treatments. At the same time, it will provide a solid theoretical basis for the research on targets of new anti-ischemic drug development with PQS and Rg1 at the center.

Materials and Methods

Drug sources

Ginseng Saponin Rg1 (Cat#: 68317. analytical standard, purity detected by high-performance liquid chromatography [HPLC] as more than 90%) was purchased from Sigma Aldrich and dissolved in dimethyl sulfoxide (DMSO) (Sigma Aldrich, Darmstadt, Germany) at 30 mg/mL as the stock solution. The working concentrations were 30 μg/mL and 100 μg/mL derived by referring to published reports (Pan *et al.*, 2000; Peng *et al.*, 2008; Wang *et al.*, 2004).

Isolation and culture of rat cortical neurons

Female Sprague-Dawley rats (16 days pregnant; obtained from Animal Experimental Center of the Second Military Medical University) were anesthetized using pentobarbital sodium, and fetuses were removed into pre-cooled Hanks' balanced salt solution (Invitrogen, Carlsbad, USA) after abdominal skin disinfection with iodine and 75% ethanol. The skin was cut and the underlying muscle and subcutaneous fascia were pulled away. Fetal cortices were dissected under a dissecting microscope and cut into pieces about 1 mm × 1 mm × 1 mm large and were digested in 0.25% trypsin-ethylenediamine tetraacetic acid (EDTA) (Invitrogen) at 37°C for 20 min. The digestion was ended by adding pre-cooled high-glucose Dulbecco minimum essential medium (DMEM) + 10% fetal bovine serum (FBS, Invitrogen) and cells were subsequently collected by centrifugation at 1000×g for 5 min, suspended in 7.5 mL DMEM with 10% FBS and seeded into 6-well plates at 2.5 mL per well (1×10^5 cells/well). The cells were incubated at 37°C in 5% CO_2, and the medium was replaced every 3 days. Cells were cultured for seven days after which they were ready to use for experiments.

Culture of 293T cells

293T cells were purchased from the Cell Bank of Chinese Academy of Sciences (Shanghai, China) and were used for packaging of recombinant lentivirus and the luciferase reporter assay. The cells were cultured in DMEM supplemented with 10% FBS at 37°C with 5% CO_2 and were passaged by trypsin digestion when confluence reached 70%.

Establishment and verification of the in vitro model of ischemic damage

To mimic the ischemic status of cells *in vivo*, primary rat cortical neurons subjected to oxygen-glucose deprivation/reperfusion (OGD/R) challenge were kept in glucose and serum-free DMEM medium under 5% CO_2 and 95% N2 for 2 h followed by 3–24 h of culture under normal conditions. Control cells were not subjected to depletion of serum and oxygen. Cell supernatants were collected at 3, 6, 12, and 24 h after depletion of serum and oxygen, and myeloperoxidase (MPO), catalase (CAT), and SOD activities were examined. Tumor necrosis factor-α (TNF-α) and interleukin-6 (IL-6) levels were assayed by Enzyme-Linked Immunosorbent Assay (ELISA). Total RNA and protein were extracted and assessed for rno-miRNA-27a-3p expression by the real-time PCR while phosphorylated p65, Caspase-3 cleaved, BCL-2, and PPARγ expression were assessed by Western blotting.

Construction of luciferase reporter vectors

The 3′-untranslated region (3′-UTR, 130 bp) of rat PPARγ was amplified from cDNA obtained through the reverse transcription of the total RNA of rat brain tissues, using the primers 5′-GCTCTAGA TGACACCTAAGAAATTTACTG TGAAAAAAGC-3′ and 5′-GCTCTAGATAGTGTGG TAATTTTTAATATTAAAAGTAA-3′. The amplification parameters were 32 cycles of denaturation at 95°C for 10 s, annealing at 58°C for 30 s, and extension at 72°C for 30 s. The product was then digested with XbaI and inserted into the pGL3-promotor vector (Promega, WI, USA). The seed region was mutated by a point mutation from 5′-ACTGTG AA-3′ to 5′-AGATCGAT-3′. The resulting vectors were named pGL3-wt-PPARγ and pGL3-mt-PPARγ.

Construction of the pcDH-miRNA-27a vector

Rat genomic DNA was extracted from rat brain tissues and used for amplification of the template (604 bp) of the precursor sequence of rno-miRNA-27a-3p. The primers used were 5′-GGAATTCTCAGACTCCAGAGTAGAGGCA GGA-3′ and 5′-CGGGATCCACTCCAGGTCTCAGTCA TGGCGGA-3′. The PCR product was digested using EcoRI and BamHI, ligated into the linear pCDH-EF1-GFP vector (System Biosciences, San Francisco, USA), and transformed into DH5α competent cells (Takara, Dalian, China). The obtained vector was called pcDH-miRNA-27.

Construction of the pSIH1-shRNA-PPARγ plasmid

A small interfering RNA (siRNA) sequence complementarily binding to the rat PPARγ sequence was chosen. The target sequences of the siRNA (5′-GTGCGATCAAAGTAGAGCC-3′) were homologous to PPARγ. The oligonucleotide templates of these shRNAs were chemically synthesized and cloned into the linear pSIH1-H1-copGFP shRNA Vector (System Biosciences), which was obtained through digestion by BamHI and EcoRI and purification by agarose gel electrophoresis. An invalid siRNA sequence (5′-GAAGCCAGATCCAGCTTCC-3′) was used as a negative control (NC). Sequencing was used to confirm the vectors constructed (pSIH1-shRNA-PPARγ and pSIH1-NC). All vectors were confirmed by DNA sequencing. Endotoxin-free DNA was prepared in all cases.

Chemical synthesis of rno-miRNA-27a-3p mimics, inhibitor and negative control

Chemically synthesized rno-miRNA-27a-mimics (5′-UUCA CAGUGGCUAAGUUCCGCtt-3′), inhibitor (5′-GCGGAA CUUAGCCACUGUGAAtt-3′), and the negative control (NC) (5′-GCUAAUGGUGCAAGUCCACAGtt-3′) were obtained from Shanghai Sangon (Shanghai, China).

Verification of the binding sites of rno-miRNA-27a-3p on the 3′-untranslated region of PPARγ mRNA by luciferase assay

TargetScan was used to predict the theoretical target (seed region) of rno-miRNA-27a-3p in the mRNA sequence of PPARγ. 293T cells were transfected with the rno-miRNA-27a-mimics, inhibitor, or NC as well as pGL-wt-PPARγ and pGL-mt-PPARγ using Lipofectamine 2000 according to the manufacturer's instructions. The cells were harvested and luciferase assays were performed 48h after transient transfection. The relative luciferase activities (ratios of firefly and renilla luciferase activity) of cell lysates were measured using a dual luciferase reporter assay system (Promega).

Lentivirus packaging

One day before transfection, 293T cells were seeded into 10-cm dishes with 1×10^6 cells/dish (Corning, NY, USA). Cotransfection of 2 μg of pCDH-miRNA-27a or pSIH1-shRNA-PPARγ or pSIH1-NC vector and 10 μg of the pPACK Packaging Plasmid Mix (System Biosciences) was done using Lipofectamine 2000 (Invitrogen) in accordance with the manufacturer's protocol. The medium was replaced with DMEM plus 1% FBS. The supernatant was harvested after 48 h and then processed by centrifugation at 5000×g at 4°C for 5 min followed by filtration through a 0.45 μm polyvinylidene difluoride (PVDF) membrane (Millipore, MI, USA). The titer of the virus was determined by gradient dilution. The packaged lentiviruses were named Lv-miRNA-27a, Lv-shRNA-PPARγ, and Lv-NC.

Lentiviral infection of rat cortical neurons

Neurons maintained in 6-well plates were divided into five groups, the cell group (not infected), the control group (infected with Lv-control), the rno-miRNA-27a-3p expression group (infected with Lv-miRNA-27a), the PPARγ silencing group (infected with Lv-shRNA-PPARγ) and the NC control group (infected with Lv-NC). Then, the medium was replaced with DMEM containing 10% FBS and 10 μl of viral solution (multiplicity of infection or MOI = 40) was added. The infection efficiency was estimated by observing the fluorescent marker 72 h after infection. Total RNA and protein were extracted from neurons 72 h after infection and assessed for rno-miRNA-27a-3p expression by

real-time PCR while phosphorylated p65, Caspase-3 cleaved, BCL-2, and PPARγ were assayed by Western blotting.

Effect of Rg1 pre-treatment on OGD damage of rat cortical neurons

The cells were divided into four groups, the control group (cultured in medium with glucose and serum, normal oxygen for 24 h), the model group (cultured in medium with vehicle, and free of glucose and serum, low oxygen for 24 h), the low-Rg1-pretreated group (pretreated with 30 μg/ml Rg1 for 24 h and cultured in medium free of glucose and serum, low oxygen for 24 h) and the high-Rg1-pretreated group (pretreated with 100 μg/ml Rg1 for 24 h and cultured in medium free of glucose and serum, low oxygen for 24 h). Cell supernatants were collected and examined for MPO, CAT, and SOD activities, as well as TNF-α and IL-6 by ELISA. In addition, apoptosis was measured by using double staining to evaluate the effect of Rg1 pre-treatment on ischemia-induced damage of rat cortical neurons.

Analysis of the mechanism by which Rg1 resists the oxygen and glucose deprivation damage

The cells were divided into the following six groups: the control group, the model group, the high-Rg1-pretreated group, the rno-miRNA-27a expression + high-Rg1-pretreated group, the high-Rg1-pretreated group with PPARγ silencing and the high-Rg1-pretreated group infected with Lv-NC. Infection was carried out 72 h before Rg1 treatment. If Rg1 inhibits ischemia-induced damage in neurons by suppressing rno-miRNA-27a-3p and consequently promoting PPARγ, then the expression of rno-miRNA-27a-3p should reverse the action of Rg1 as would PPARγ knockdown. The evaluation of damage induced by ischemia was based on the examination of phosphorylated p65, caspase-3 cleaved and BCL-2 levels, and cell viability.

Cellular proliferation assay

The Cell Counting Kit-8 (CCK-8) is an effective approach for evaluating cell proliferation, which is an important index of cellular function. Briefly, cells were seeded in 96-well plates at a density of 1×10^5 cells per well. 10 μl of CCK-8 solution (Dojindo, Japan) was added and the cells were then cultured under normal conditions for an additional 4 h before measurement of absorbance at 490 nm (Multiskan FC, Thermo Fisher Scientific, Carlsbad, CA, USA).

Detection of apoptosis

Cells were seeded in 6-well plates at a density of 5×10^5 cells per well. The cells were collected and measured for apoptosis using flow cytometry (FACS Calibur, BD) employing the Annexin V: FITC Apoptosis Detection Kit II (Cat: 556570, BD). Cells were suspended by trypsinization and washed with Dulbecco's Phosphate-Buffered Sallines (dPBS) and subsequently suspended in 500 μl binding buffer. Addition of 5 μl of annexin was done at with V-FITC in dark for 10 min. Cells were then stained with 5 μl Propidium Iodide for 5 min. Apoptosis was analyzed on BD-FACS Calibur using the FITC (FL1) channel and the PI (FL2) channel at an excitation wavelength of 488 nm.

Assays for measuring myeloperoxidase, catalase and superoxide dismutases activities

Cell supernatants were harvested and cell debris was removed by centrifugation at 3000×g after which MPO, CAT, and SOD activities were examined by using corresponding detection kits following the manufacturer's instructions. All kits, including the catalase assay kit (CAT100), the MPO fluorometric activity assay kit (MAK069), and the SOD determination kit (19160) were purchased from Sigma Aldrich.

Measurement of tumor necrosis factor-alpha and interleukin-6 by ELISA

Cell supernatants were harvested and cell debris was removed by centrifugation at 3000×g. TNF-α and IL-6 levels were assayed by using ELISA kits following the manufacturer's instructions. The kits, including the Rat TNF-α ELISA Kit (KRC-3011) and the Rat IL-6 Immunoassay (R6000B), were purchased from Invitrogen.

Measurement of rno-miRNA-27a-3p levels

To measure the level of rno-miRNA-27a-3p, total RNA (2 μg) was used for cDNA preparation with an M-MLV reverse transcription kit and the following specific primers, rat U6 snRNA (NM_001101.3): 5′-AAAATATGAACGCTTCACG-3′, and rno-miRNA-27a-3p: 5′-GTCGTATCCAGTGCGTG TCGTGGAGTCGGCAATTGCACTGGATACGACGCGGA A-3′. RNA contents were detected using fluorescent dye PCR (Takara BIO) following the manufacturer's instructions. The following primers were used for quantification of rat U6 snRNA and rno-miRNA-27a-3p: U6 snRNA: 5′-GTGCCTG CTTCGGCAGCACATATA-3′ and 5′-AAAATATGAACG CTTCACG-3′, which produced a segment of 107 bp; and rno-miRNA-27a-3p: 5′-TTCACAGTGGCTAAGTTCCGC-3′ and 5′-GTCGTATCCAGTGCGTGTCGTG-3′, which produced a segment of 70 bp. The PCR system mix included the Takara SYBR Premix Ex Tap 10 μl, forward and reverse primers (20 μM) 0.2 μl each, and cDNA 2 μl with dH2O added to a final volume of 20 μl. The cycling parameters were 40 cycles of denaturation at 95°C for 10 s, annealing at 60°C for 20 s, and extension at 72°C for 20 s. U6 small nuclear RNA (snRNA) was used as a reference to normalize the miRNA-27a level using the $2^{-\Delta\Delta Ct}$ method. Each RNA sample was run in triplicate.

Protein detection

Protein was extracted from the cells using the M-PER mammalian protein extraction reagent (Pierce, IL, USA). Equal amounts of protein (15 μg per lane), as estimated by a bicinchoninic acid (BCA) protein assay kit (Pierce), were loaded onto (11%) sodium dodecyl sulfate polyacrylamide gel electrophoresis (SDS-PAGE) gels and transferred onto nitrocellulose membranes. The blots were probed with monoclonal antibodies against rat PPARγ (1:500), P-p65 (1:300), P65 (1:500), Caspase-3 (1:200), Caspase-3 cleaved (1:600), BCL-2(1:600) and beta-actin (1:1200) (Santa Cruz, USA), followed by incubation with the secondary HRP-conjugated anti-mouse/rabbit antibody (Santa Cruz). After washing, bands were detected by chemiluminescence and

imaged with X-ray films. β actin was used as an endogenous reference for normalization.

Data analysis

All data were expressed as the mean ± standard deviation (SD) and were analyzed by one-way analysis of variance (ANOVA). The Least Significant Difference (LSD) was used for multiple comparisons between any two means. p-values < 0.05 were considered statistically significant. All statistical analysis was performed using the SPSS 13.0 software.

Results

Establishment and verification of the in vitro oxygen and glucose deprivation model

To verify the *in vitro* ischemia model, we performed a comprehensive study on cellular injuries. The results of the quantitative analysis of MPO, CAT, and SOD activities are shown in Fig. 1A. The activities of CAT and SOD in the OGD model group were higher than those of the control group (p < 0.05, *vs.* the control group) at 3 h. Decreasing

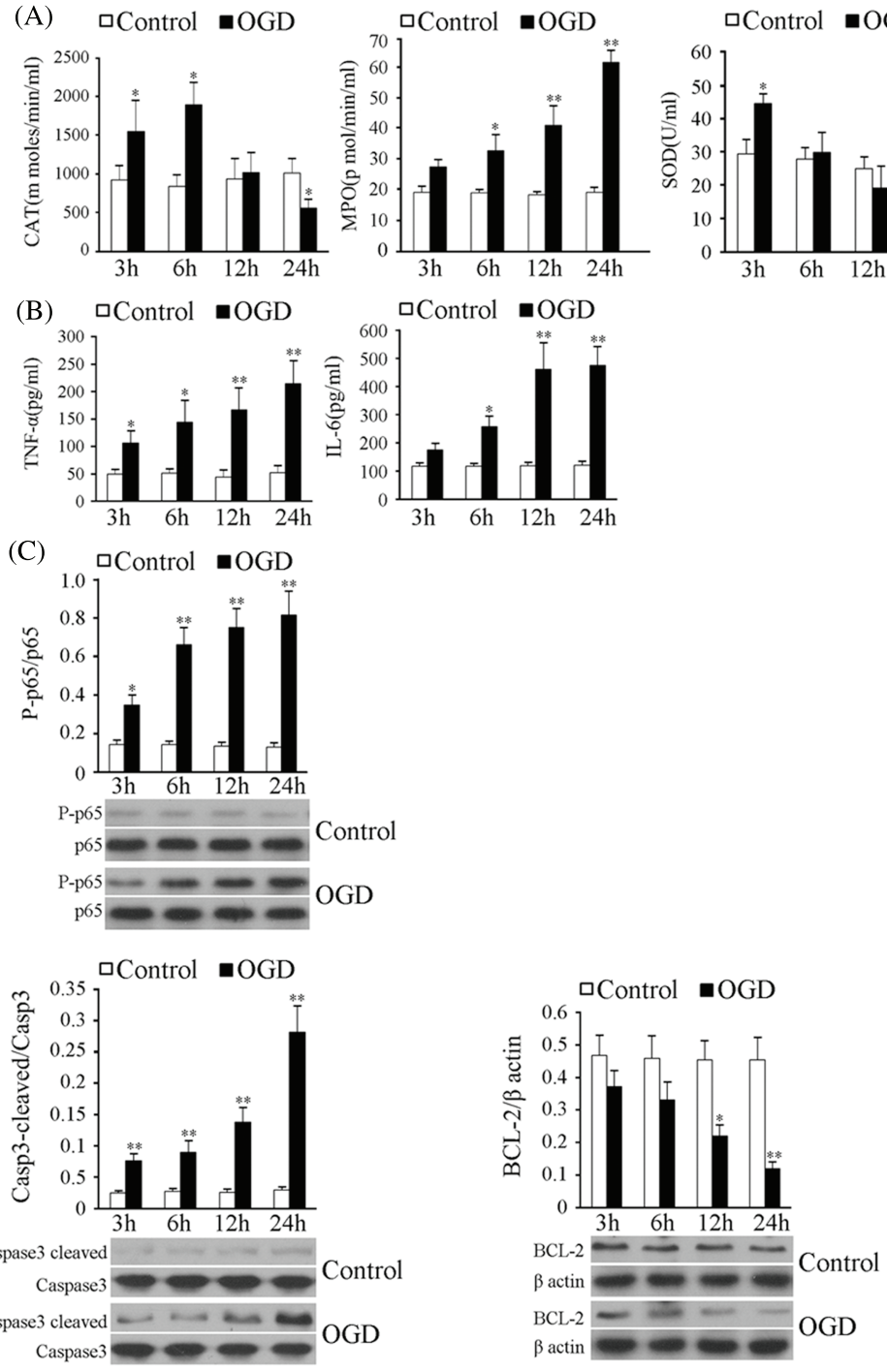

FIGURE 1. Measurement of indices of ischemic damage in the *in vitro* model of cerebral ischemia. (A) Left, middle and right panels show the myeloperoxidase (MPO), catalase (CAT), and superoxide dismutase (SOD) activities of neuronal supernatants subjected to glucose-and-serum-free and low-oxygen treatment for 3–24 h. (B) Tumor necrosis factor-alpha (TNF-α) and interleukin-6 (IL-6) levels of neurons subjected to the glucose-and-serum-free and low-oxygen treatment for 3–24 h. (C) Phosphorylated p65, cleaved Caspase-3 and BCL-2 levels in neurons subjected to the OGD treatment for 3–24 h. Results represent means ± SD of at least three separate experiments. The samples were derived from the same experiment and the gels/blots were processed in parallel. $^{**}p$ < 0.01, $^{*}p$ < 0.05, when compared to the control group at the same time point.

over time until they were lower than in the control group ($p < 0.05$, *vs.* the control group) at 24 h. At the four time points, the MPO activity in the OGD model group increased over time, becoming significantly higher than the control group at 6, 12, and 24 h ($p < 0.05$, *vs.* the control group). These changes in these three biochemical indexes were consistent with the characteristics of ischemic damage. TNF-α and IL-6 are two typical inflammatory factors that can be used to characterize the degree of inflammation. As shown in Fig. 1B, between 3 and 24 h, TNF-α and IL-6 levels in supernatants increased over time, becoming significantly higher than the control group at all time points for TNF-α and at 6, 12, and 24 h for IL-6 ($p < 0.05$, *vs.* the control group). Fig. 1C shows the profile of three proteins involved in the apoptosis pathway. Phosphorylated p65 of NF-κB was increased over time, becoming significantly higher than the control group ($p < 0.05$, *vs.* the control group). A similar trend was observed for cleaved caspase-3 at all the time points, indicating that in the OGD model, the activity of caspase-3 was increased. Data also showed that BCL-2, an important index for the proliferation of cells, was decreased over time between 3 and 24 h after the establishment of the model, becoming lower than in the control group at 12 and 24 h ($p < 0.05$, *vs.* the control group). These results indicated that the *in vitro* model of cortical nerve ischemia injury was successfully established.

Effect of oxygen and glucose deprivation on rno-miRNA-27a-3p and peroxisome proliferator-activated receptor gamma expression in rat cortical neurons

The RT-qPCR data showed that OGD treatment could gradually enhance the expression of rno-miRNA-27a-3p within 24 h, and it was significantly higher than that of the control group at 6, 12 and 24 h ($p < 0.05$, *vs.* the control group) (Fig. 2A). As shown in Fig. 2B, the expression of PPARγ protein was gradually reduced by the OGD treatment within 24 h, and it was significantly lower than that of the control group at 12 and 24 h ($p < 0.05$, *vs.* the ontrol group) (Fig. 2B). The RT-qPCR data also showed that the relative mRNA level of PPARγ was gradually reduced by OGD treatment within 24 h, but the difference was statistically significant only at the 24 h point ($p < 0.05$, *vs.* the control group) (Fig. 2C). This suggests that under OGD conditions, the decrease of PPARγ expression in rat cortical neurons is likely to occur at the post-transcriptional level (mRNA changes lag behind that of the protein). The regulation of a target gene by miRNA is a typical post-transcriptional regulation mechanism. Thus, whether the decrease of the PPARγ protein expression is directly caused by the decrease of the rno-miRNA-27a-3p level was undoubtedly worthy of our further attention.

rno-miRNA-27a could inhibit the translation of peroxisome proliferator-activated receptor gamma mRNA by binding to its 3′UTR

The bioinformatics analysis (Fig. 3A) showed that there is a binding site (5′-ACUGUGAA-3′) for the seed region of rno-miRNA-27a in the 3′-UTR of the PPARγ mRNA. The luciferase assay data 48 h after transfection (Fig. 3B) showed that the rno-miRNA-27a-mimic significantly inhibited the activity of luciferase in the 293T cells transfected with pGL3-wt-PPARγ from 28.12 ± 7.31 to 12.16 ± 0.24 ($p < 0.01$). The rno-miRNA-27a-inhibitor increased the luciferase activity from 28.12 ± 7.31 to 42.31 ± 6.61 in pGL3-wt-PPARγ

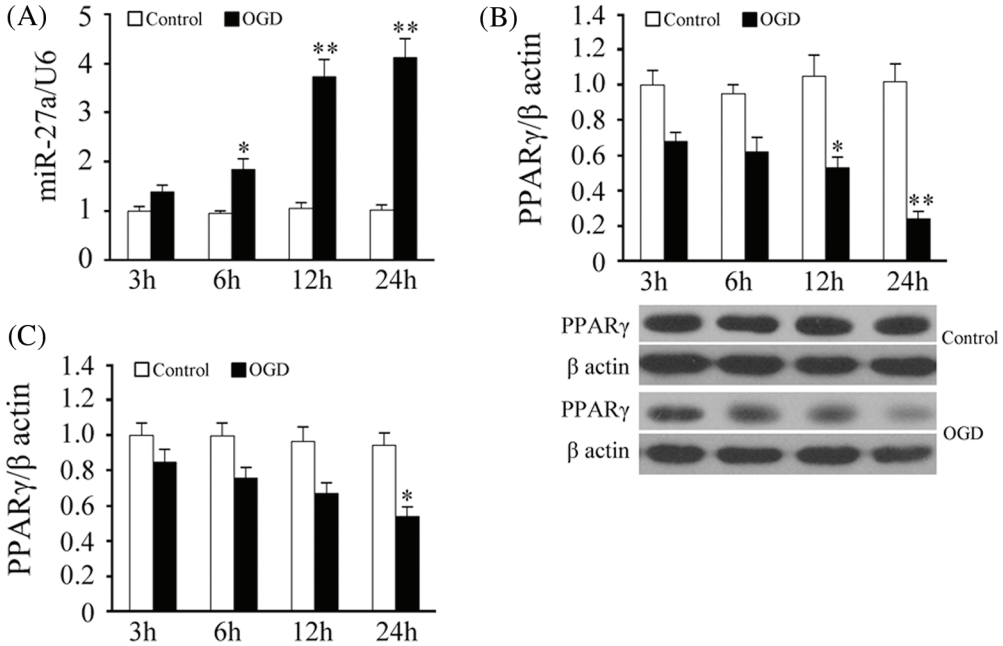

FIGURE 2. Effect of oxygen and glucose deprivation on rno-miRNA-27a-3p and peroxisome proliferator-activated receptor gamma expression in rat cortical neurons. (A) rno-miRNA-27a-3p levels in neurons subjected to glucose-and-serum-free and low-oxygen treatment for 3–24 h, U6 was used as the internal reference. (B) Peroxisome proliferator-activated receptor gamma (PPARγ) protein levels in neurons subjected to the glucose-and-serum-free and low-oxygen treatment for 3–24 h. Upper, density analysis, and lower, target band scanned. (C) PPARγ mRNA levels in neurons subjected to glucose-and-serum-free and low-oxygen treatment for 3–24 h, β-actin was used as the reference. Results represent means ± SD of at least three separate experiments. The samples were derived from the same experiment and the gels/blots were processed in parallel, $^{**}p < 0.01$, $^{*}p < 0.05$, when compared to the control group at the same time point.

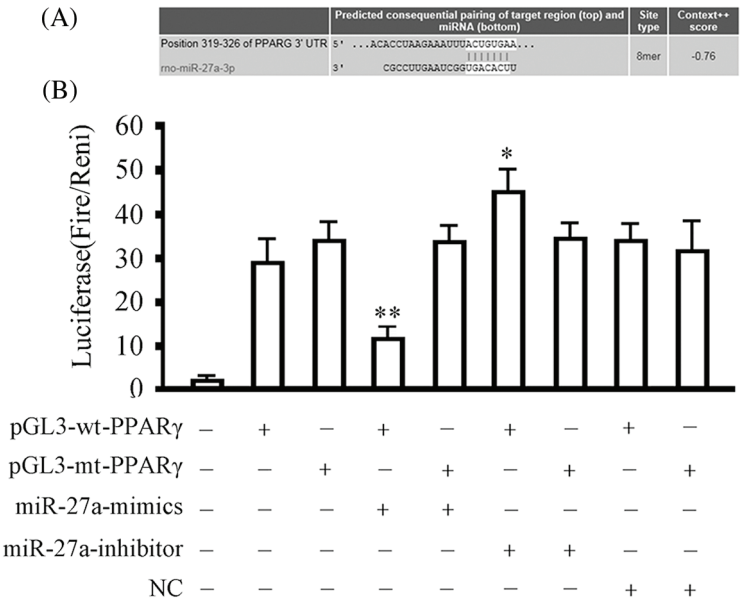

FIGURE 3. rno-miRNA-27a-3p binds to peroxisome proliferator-activated receptor gamma at the 3′-untranslated region. 293T cells were transfected with the indicated vectors and subjected to luciferase activity assay 48 h later. Data are expressed as mean ± SD of at least three independent experiments. *$p < 0.05$, and **$p < 0.01$, compared with the group transfected with the same vector but without the rno-miRNA-27a-3p mimics or inhibitor. (A) Schematic representation of rno-miRNA-27a-3p binding to the 3′-untranslated region (UTR) of peroxisome proliferator-activated receptor gamma (PPARγ). (B) The relative luciferase activity assay results.

transfected 293T cells ($p < 0.05$). For the mutant luciferase vector, pGL3-mt-PPARγ transfected 293T cells, neither pGL3-wt-PPARr nor pGL3-wt-PPARdidnothavean effect on the intracellular luciferase activity ($p > 0.05$).

Overexpression of miRNA-27a-3p and silencing of peroxisome proliferator-activated receptor gamma in rat cortical neurons

As we all know, it is difficult to obtain high gene transfer efficiency through conventional transfection methods in cortical neurons. However, the stability and effectiveness of gene intervention is the most basic requirement in gene functional research. In this study, we successfully solved the problem of such transfection challenges to the primary cortical neurons by using the lentivirus-based approach. As shown in Fig. 4A, the infection efficiency of lentivirus in cortical neurons was greater than 90% according to the fluorescent marker GFP 72 h after infection. Examination of rno-miRNA-27a-3p levels (Fig. 4B) demonstrated that the level of rno-miRNA-27a-3p increased by 4.21 times in the Lv-miRNA-27a infected cortical neurons ($p < 0.01$, *vs.* the cell group), Western blotting showed that the expression of the PPARγ protein was reduced by about 0.11 times in the Lv-shRNA-PPARγ infected cortical neurons ($p < 0.01$, *vs.* the cell group) and was reduced by 0.19 times in Lv-miRNA-27a-infected cortical neurons ($p < 0.01$, *vs.* the cell group) 72 h after infection. There was no difference in the expression of rno-miRNA-27a-3p and PPARγ protein in the cell group, the Lv-control group, and the Lv-NC group ($p > 0.05$). The above results show that the overexpression of rno-miRNA-27a-3p could significantly inhibit the expression of PPARγ protein, but PPARγ gene silencing had no effect on rno-miRNA-27a-3p. This indicated that the upstream and downstream relationship between them completely conforms to the theoretical prediction of the regulation of PPARγ by rno-miRNA-27a-3p.

Rg1 pre-treatment could significantly alleviate ischemic injury in neurons in vitro

The quantitative analysis of oxidation indices (CAT, SOD) and inflammatory markers (MPO, TNF-α, and IL-6), shown in Figs. 5A and 5B, respectively, demonstrated that pre-treatment of Rg1 at low or high doses for 24 h significantly inhibited the changes induced by ischemia in rat cortical neurons. Further, pre-treatment of Rg1 at 100 μg/ml could significantly inhibit the apoptosis of rat cortical neurons induced by OGD ($p < 0.01$, *vs.* the control group) (Fig. 5C).

Validation of the specificity of the rno-miRNA-27a/peroxisome proliferator-activated receptor gamma pathway

As it is important to study whether the rno-miRNA-27a/PPARγ pathway is critical in the inhibition of ischemic damage in neurons by Rg1, we subsequently investigated the role of the pathway. OGD treatment for 24 h increased rno-miRNA-27a-3p levels in neurons by 6.31 fold ($p < 0.01$, *vs.* the control group) which was reversed by pre-treatment with 100 μg/ml Rg1 ($p < 0.01$, *vs.* the OGD group). Lv-miRNA-27a infection significantly increased the level of rno-miRNA-27a-3p in neurons in the Rg1+OGD group. However, Lv-shRNA-PPAR had no significant effect on the relative content of rno-miRNA-27a-3p in the neurons of the Rg1+OGD group ($p < 0.05$) (Fig. 6A). The CCK-8 analysis results showed that OGD for 24 h evidently inhibited the proliferation of neurons ($p < 0.01$, *vs.* the control group, 72 h) which was reversed by pre-treatment of Rg1 at 100 μg/ml ($p < 0.01$, *vs.* the OGD group, 72 h). The results also showed that both rno-miRNA-27a-3p overexpression and PPARγ silencing could reverse the above effects of Rg1 ($p < 0.01$, *vs.* the Rg1+OGD group, 72 h) (Fig. 6B). As shown in Fig. 6C, the expression of PPARγ and Bcl-2 proteins were negatively correlated with that of rno-miRNA-27a-3p while phosphorylated p65 and cleaved

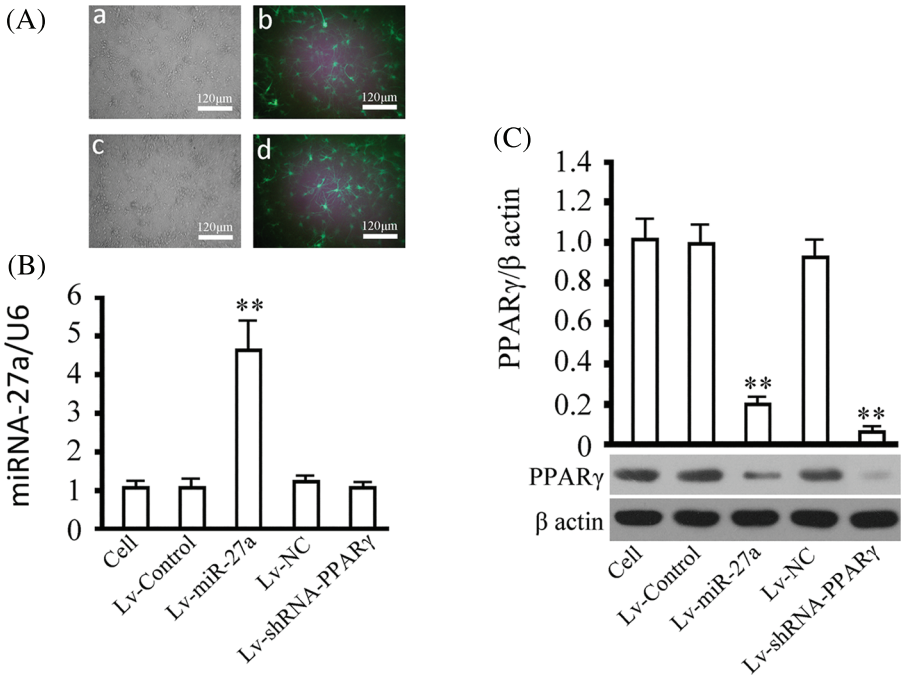

FIGURE 4. Overexpression of rno-miRNA-27a-3p and silencing of peroxisome proliferator-activated receptor gamma (PPARγ) by the lentiviral approach. (A) Neurons infected with lentivirus were observed for the determination of the gene delivery efficiency according to the ratio of green fluorescent protein-expressing cells to the total cells. a and c represent bright-field microscopy images and b and d represent fluorescent-light microscopy images. a and b indicate neurons infected with Lv-miRNA-27a, and c and d neurons infected with Lv-shRNA-PPARγ, multiplicity of infection (MOI) = 40, at a magnification of 120×. (B) miRNA-27a expression was measured in cells infected with the indicated virus. (C) PPARγ expression was examined in the cells infected with the indicated virus, beta actin was used as an internal reference. Results represent means ± SD of at least three separate experiments. The samples were derived from the same experiment and the gels/blots were processed in parallel. $^{**}p < 0.01$, $^{*}p < 0.05$, when compared to the control group (cells without infection).

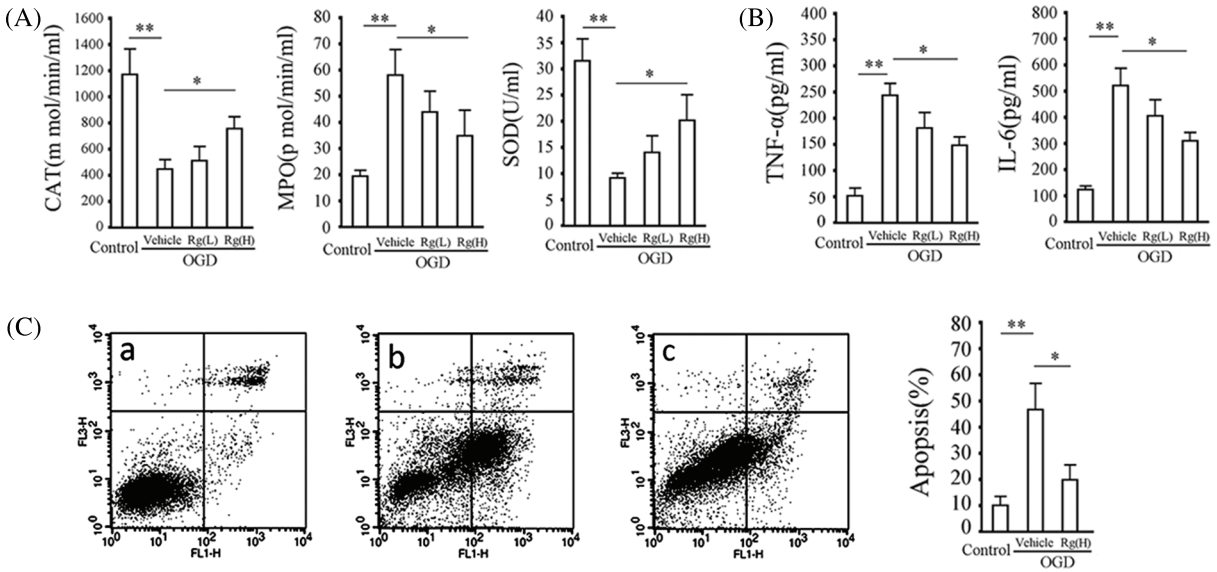

FIGURE 5. Rg1 alleviates changes in indices of ischemic damage in neurons. (A) Left, middle and right show the myeloperoxidase (MPO), catalase (CAT), and superoxide dismutase (SOD) activities in the supernatants of the neurons pretreated with or without Rg1 and subsequently subjected to the glucose-and-serum-free and low-oxygen treatment for 24 h. (B) Tumor necrosis factor-alpha (TNF-α) and interleukin-6 (IL-6) levels in the supernatants of the neurons pre-treated with or without Rg1 and subsequently subjected to glucose-and-serum-free and low-oxygen treatment for 24 h. (C) Apoptosis assay. Left: flow cytometry results, a, b, and c are the cell control, model group and group pretreated with 100 μg/ml Rg1, respectively. x and y coordinates represent fluorescein isothiocyanate (FITC) and propidium iodide (PI) staining, respectively. The right lower quadrant represents the cells in the earlier stages of apoptosis and the right upper quadrant represents the cells in the later stages of apoptosis. Right, data obtained from apoptotic cells, x and y coordinates include cells grouped from the earlier and later stages of apoptosis. Results represent means ± SD of at least 3 separate experiments. $^{**}p < 0.01$, $^{*}p < 0.05$, when compared to the control group or vehicle group.

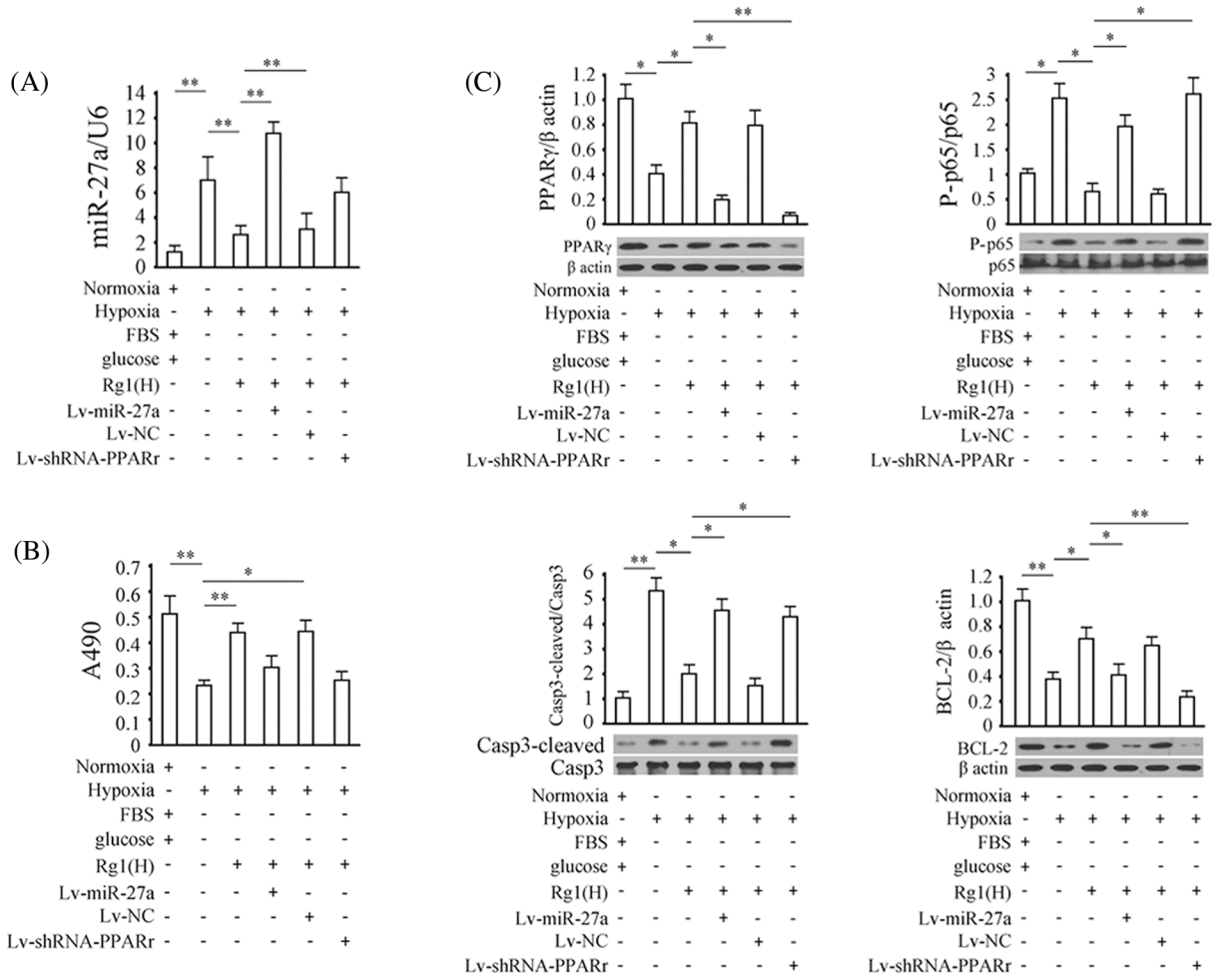

FIGURE 6. Validation of the specificity of the rno-miRNA-27a-3p/PPARγ pathway. (A) rno-miRNA-27a-3p levels in different groups, U6 was used as the internal reference. (B) Cell proliferation data. x and y coordinates represent grouped cells and absorbance values read at A490 (in proportion to cell viability). (C) Levels of phosphorylated p65, cleaved Caspase-3, B-cell Lymphoma-2 (BCL-2), and peroxisome proliferator-activated receptor gamma (PPARγ) in neurons subjected to the indicated treatments. Results represent means ± SD of at least three separate experiments. The samples were derived from the same experiment and the gels/blots were processed in parallel.

Caspase-3 were negatively correlated with PPARγ and rno-miRNA-27a-3p in all groups (Fig. 6C).

Discussion

Ischemic cerebrovascular disease (ICVD) accounts for approximately 15% percent of cerebrovascular diseases. As the aging population grows, ICVD has become one of the most common illnesses to cause serious harm to human health, due to its rising morbidity. Currently, treatments for ICVD include thrombolytic therapy and neuroprotective treatments. Thrombolytic therapy cannot be widely used in clinical practice due to narrow treatment time windows and complications caused by excessive bleeding. A limitation of neuroprotectants is that they are still in the experimental stage. Thus, it is necessary to find effective and safe new drugs to enhance the quality of life of patients with ICVD.

Recent studies have found that cerebral ischemic injury is a complex process with multiple components and mechanisms involving inflammation, oxidative stress, and apoptosis (Khoshnam *et al.*, 2017; Wu *et al.*, 2020). Therefore, inhibiting the inflammatory response, suppressing the oxidative stress, and resisting apoptosis are important strategies for therapies against ICVD. Peroxisome proliferator-activated receptors (PPARs) (Tyagi *et al.*, 2011), transcription factors, and members of the nuclear receptor superfamily, are usually divided into three subtypes, PPARα, PPARβ/δ, and PPARγ. They are found in a wide variety of tissues including central nervous tissues (Schnegg and Robbins, 2011). Recently, many studies have substantiated the role of PPARγ in cerebral ischemia (Villapol, 2018; Zeng *et al.*, 2012). PPARγ may be a new target for ICVD as its agonists were shown to alleviate brain damage by inhibiting inflammation, reducing oxidative stress, improving neurological function, and inhibiting apoptosis (Boujon *et al.*, 2019; Chen *et al.*, 2012b; Kaundal and Sharma, 2011a, 2011b).

Hundreds of miRNAs have been identified in recent years. They function as important regulators in physiological processes, including the embryonic development of the nervous system, nerve cell differentiation, synaptic connections, dendritic spine formation, and neuroprotection (Nowak and Michlewski, 2013). Some miRNAs play a role in nervous system diseases such as brain tumors, Alzheimer's disease, Parkinson's disease, and stroke (Dehghani *et al.*, 2018; Mirzaei *et al.*,

2018; Petrescu *et al.*, 2019; Singh and Sen, 2017). Therefore, clarifying the regulatory mechanisms of miRNAs is of great importance for understanding the pathogenesis of ischemic cerebrovascular diseases and the in-depth study of miRNAs' regulatory functions. In our previous study, we found that rno-miRNA-27a-3p expression was significantly upregulated under ischemic conditions based on miRNA chip technology and real-time PCR (Zhai *et al.*, 2012; Zhang *et al.*, 2012). Wang *et al.* (2012b) proved that PPARγ was a target of miRNA-27b. Further, overexpression of miRNA-27b significantly decreased PPARγ levels while the knockdown of the miRNA increased PPARγ expression (Wang *et al.*, 2012b). Karbiener *et al.* (2009) also further showed that miRNA-27b targeted PPARγ. miRNA-27b and miRNA-27a belong to the same cluster of genes and may have similar capabilities. Based on the aforementioned evidence, we speculated that rno-miRNA-27a might target PPARγ to regulate its roles in inflammation, oxidative stress, apoptosis, and the regulation of cerebral ischemic injury. According to a review of the literature, rno-miRNA-27a-3p is located on chromosome 11. Human miRNA-27a was able to regulate ischemia-induced injury in cerebral neurons in one study (Sepramaniam *et al.*, 2014).

The mechanisms of ICVD are complex due to the interaction of various factors. Therefore, single-target treatments often offer little effect. Chinese traditional medicine is characterized by multi-faceted and prominent synergistic effects which have demonstrated benefits for ischemic stroke. MiRNAs, which modulate gene expression and protein translation, may be effective targets for cerebral ischemic injury. For example, the miR-106b-5p antagomir has been shown to inhibit the apoptosis in neurocytes induced by cerebral ischemia (Li *et al.*, 2017b). In another study, the knockdown of microRNA-383 ameliorated injury after cerebral ischemia by targeting PPARγ (Pei *et al.*, 2016). Further, Cai *et al.* (2016) studied the inhibition of neuronal apoptosis by miRNA-27a in an OGD model, suggesting that miRNA-27a may be a potential target for the treatment of neonatal hypoxic-ischemia encephalopathy. In the present study, for the first time, we associate the inhibition of ischemic injury by Rg1 through PPARγ with the regulation of rno-miRNA-27a-3p. This may help explain how Rg1 alleviates cerebral ischemic injury and allow the development of a novel therapeutic approach. Our results showed that the rno-miRNA-27a-3p/PPARγ axis is involved in cortical neuron injury induced by ischemia. Further, Rg1 pre-treatment could indirectly up-regulate the expression of PPARγ protein by down-regulating rno-miRNA-27a-3p, thus effectively inhibiting inflammatory reaction, oxidative stress and apoptosis in rat cortical neurons exposed to OGD. In the validation of the pathway involving Rg1, as the reply control for the path-leading demonstration, both the overexpression of exogenous rno-miRNA-27a-3p and the silencing of endogenous PPARr could reverse the role of Rg1 in protecting against neuronal damage by OGD. This indicated that the effect of Rg1 on cerebral ischemia injury depends on the regulation of the rno-miRNA-27a-3p/PPARr pathway.

We identified rno-miRNA-27a-3p as an effective target of Rg1 yielding neuroprotective effects against cerebral ischemia. This provides new molecular targets for novel therapies and drug screening. We also obtained some clues from current data which imply that rno-miRNA-27a is regulated by Rg1 at the level of transcription. In this study, Rg1 significantly inhibited intracellular rno-miRNA-27a-3p. When we increased the expression of exogenous rno-miRNA-27a-3p, mature rno-miRNA-27a-3p was highly expressed in the Rg1 pre-treated group, suggesting that Rg1 had little effect on exogenous rno-miRNA-27a-3p. What makes an exogenous expression system different from an endogenous expression system is that endogenous rno-miRNA-27a-3p includes a wild-type promoter while exogenous rno-miRNA-27a-3p entails a eukaryotic promoter. Thus, there may be some crucial transcription factors shared between the rno-miRNA-27a promoter and Rg1 that bind to the promoter region of rno-miRNA-27a-3p and work as targets of Rg1. When Rg1 is combined with those transcription factors, the transcription of rno-miRNA-27a-3p might be influenced. Finally, this work lays the groundwork for a proposed long-term project. Crucial to this is the selection of transcription factors regulated by Rg1 by high-throughput screening methods and the use of drug affinity responsive target stability (DARTS) (Kim *et al.*, 2020) and co-localization analysis to define the relationship between Rg1 and the screened transcription factors. In addition, predicting the binding site of transcription factors on the rno-miRNA-27a-3 promoter and analyzing the binding site according to luciferase reporter and CHIP-PCR are also planned. This would allow for more accurate assessments of the mechanisms of Rg1-related pathways in alleviating ischemic injury. Although there is still a lot of work to be done, this study provides important guidance for revealing the target genes of ischemic injury and the mechanisms of the therapeutic effects at the miRNA level. Cerebral ischemia injury can lead to extensive changes in the expression of miRNA in the brain of rats. To summarize, this study was mainly aimed at rno-miRNA-27a-3p in regulating its target gene PPARγ, thereby affecting the expression of PPARγ and playing a protective role against cerebral ischemia injury. The study of other miRNAs in the pathogenesis of cerebral ischemic injury remains to be done in depth.

In conclusion, this study preliminarily clarified the mechanism of Rg1 in resisting cortical neuron damages (such as the release of inflammatory factors, the increase in oxidative stress, the reduction of proliferative activity, and the increase of apoptosis, etc.) induced by cerebral ischemia. This provides a theoretical basis for the clinical formulation of ischemic brain injury treatment based on Rg1. Although the interaction between Rg1 and rno-miRNA-27a-3p still needs systematic studies, this finding is still major progress in the target and pathway analysis of PQS/Rg1 as an anti-ischemic approach.

Acknowledgement: We thank all colleagues from the departments of all authors of this paper.

Funding Statement: The project was financially supported by the National Natural Science Foundation of China, Nos. 81973317, 81374007, 81870977; the Natural Science

Foundation of Heilongjiang Province, HL2019H062; the Projects of Basic Scientific Research Business Expenses in Higher Education Institutions of Heilongjiang Province, No. 2018-KYYWF-MY-005; and the Students Innovative and the Entrepreneurship Training Scientific Research Foundation of Heilongjiang Province, No. 102292017001.

Author Contributions: Ting-ting Zhang, Jia-nan Yu, Yue Guan, and Feng-guo Zhai designed, performed the experiments, and wrote the manuscript. Wen-yuan Li, Jia-wei Liu, Yu-jia Zheng, Yan-zhong Guan, Hui-lin Guan, and Li-xin Guan performed the experiments, collected the data, and analyzed the data. All authors have read and approved the manuscript.

Availability of Data and Materials: The dataset(s) supporting the conclusions of this article are available from the corresponding author upon reasonable request.

Ethics Approval: All experimental procedures described in this manuscript were approved by the Experimental Animal Ethics Committee of the Mudanjiang Medical University and experiments involving animals comply with the ARRIVE guidelines from the NC3Rs (National Centre for the Replacement, Refinement & Reduction of Animals in Research).

Conflicts of Interest: The authors declare that they have no conflicts of interest to report regarding the present study.

References

Ahuja A, Kim JH, Kim JH, Yi YS, Cho JY (2018). Functional role of ginseng-derived compounds in cancer. *Journal of Ginseng Research* **42**: 248–254. https://doi.org/10.1016/j.jgr.2017.04.009

Boujon V, Uhlemann R, Wegner S, Wright MB, Laufs U, Endres M, Kronenberg G, Gertz K (2019). Dual PPARα/γ agonist aleglitazar confers stroke protection in a model of mild focal brain ischemia in mice. *Journal of Molecular Medicine* **97**: 1127–1138. https://doi.org/10.1007/s00109-019-01801-0

Cai Q, Wang T, Yang WJ, Fen X (2016). Protective mechanisms of microRNA-27a against oxygen-glucose deprivation-induced injuries in hippocampal neurons. *Neural Regeneration Research* **11**: 1285–1292. https://doi.org/10.4103/1673-5374.189194

Chen Y C, Wu JS, Tsai HD, Huang CY, Chen JJ, Sun GY, Lin TN (2012b). Peroxisome proliferator-activated receptor gamma (PPAR-γ) and neurodegenerative disorders. *Molecular Neurobiology* **46**: 114–124. https://doi.org/10.1007/s12035-012-8259-8

Dehghani R, Rahmani F, Rezaei N (2018). MicroRNA in Alzheimer's disease revisited: Implications for major neuropathological mechanisms. *Reviews in the Neurosciences* **29**: 161–182. https://doi.org/10.1515/revneuro-2017-0042

Feng R, Liu J, Wang Z, Zhang J, Cates C, Rousselle T, Meng Q, Li J (2017). The structure-activity relationship of ginsenosides on hypoxia-reoxygenation induced apoptosis of cardiomyocytes. *Biochemical and Biophysical Research Communications* **494**: 556–568. https://doi.org/10.1016/j.bbrc.2017.10.056

Guan LX (2008). Protective effects of Panax quinquefolium saponins from stems and leaves (PQS) on focal cerebral ischemia damage and its mechanism. *Heilongjiang University of Chinese Medicine* **28**: 5. https://doi.org/10.7666/d.y1375323

Jian R, Yang M, Xu F (2019). Lentiviral-mediated silencing of mast cell-expressed membrane protein 1 promotes angiogenesis of rats with cerebral ischemic stroke. *Journal of Cellular Biochemistry* **120**: 16786–16797. https://doi.org/10.1002/jcb.28937

Karbiener M, Fischer C, Nowitsch S, Opriessnig P, Papak C, Ailhaud G, Dani C, Amri EZ, Scheideler M (2009). microRNA miR-27b impairs human adipocyte differentiation and targets PPARγ. *Biochemical and Biophysical Research Communications* **390**: 247–251. https://doi.org/10.1016/j.bbrc.2009.09.098

Kaundal RK, Sharma SS (2011a). Ameliorative effects of GW1929, a nonthiazolidinedione PPARγ agonist, on inflammation and apoptosis in focal cerebral ischemic-reperfusion injury. *Current Neurovascular Research* **8**: 236–245. https://doi.org/10.2174/156720211796558078

Kaundal RK, Sharma SS (2011b). GW1929: A nonthiazolidinedione PPARγ agonist, ameliorates neurological damage in global cerebral ischemic-reperfusion injury through reduction in inflammation and DNA fragmentation. *Behavioural Brain Research* **216**: 606–612. https://doi.org/10.1016/j.bbr.2010.09.001

Khoshnam SE, Winlow W, Farzaneh M, Farbood Y, Moghaddam HF (2017). Pathogenic mechanisms following ischemic stroke. *Neurological Sciences* **38**: 1167–1186. https://doi.org/10.1007/s10072-017-2938-1

Kim Y, Sugihara Y, Kim TY, Cho SM, Kim JY, Lee JY (2020). Identification and validation of VEGFR2 kinase as a target of voacangine by a systematic combination of DARTS and MSI. *Biomolecules* **10**: 508. https://doi.org/10.3390/biom10040508

Li Y, Guan Y, Wang Y, Yu CL, Zhai FG (2017c). Neuroprotective effect of the ginsenoside Rg1 on cerebral ischemic injury *in vivo* and *in vitro* is mediated by PPARγ-regulated antioxidative and anti-inflammatory pathways. *Evidence-Based Complementary and Alternative Medicine* **2017**: 7842082. https://doi.org/10.1155/2017/7842082

Li ZN, Guan LX, Wei XG, Jiao GY, Su YM (2010). The effect of Panax quinquefolium saponins on caspase-9 on cerebral ischemia. *Journal of Chengdu Medical College* **5**: 3.

Li P, Shen M, Gao F, Wu J, Zhang J, Teng F, Zhang C (2017b). An antagomir to MicroRNA-106b-5p ameliorates cerebral ischemia and reperfusion injury in rats via inhibiting apoptosis and oxidative stress. *Molecular Neurobiology* **54**: 2901–2921. https://doi.org/10.1007/s12035-016-9842-1

Li JP, Yuan Y, Zhang WY (2017a). Influence of Panax quinquefolium saponins on oxidative damage and function of vascular endothelium in diabetic rats. *Chinese Pharmacological Bulletin* **33**: 1698–1702.

Liu HY (2014). Research progress of Xinyue capsule for the prevention and treatment of coronary heart disease. *Shanghai Medical Journal* **15**: 1–4.

Liu M, Wang C, Wang XR, Song DD, Liu XH, Shi DZ (2013). Panax quinquefolium saponin attenuates ventricular remodeling after acute myocardial infarction in rats by inhibiting endoplasmic reticulum stress-related apoptosis. *Chinese Journal of Pathophysiology* **29**: 796–803. https://doi.org/10.3969/j.issn.1000-4718.2013.05.005

Mirzaei H, Momeni F, Saadatpour L, Sahebkar A, Goodarzi M, Masoudifar A, Kouhpayeh S, Salehi H, Mirzaei HR, Jaafari MR (2018). MicroRNA: Relevance to stroke diagnosis,

prognosis, and therapy. *Journal of Cellular Physiology* **233**: 856–865. https://doi.org/10.1002/jcp.25787

Nowak JS, Michlewski G (2013). miRNAs in development and pathogenesis of the nervous system. *Biochemical Society transactions* **41**: 815–820. https://doi.org/10.1042/BST20130044

Pan S, Liu D, Zheng S (2000). The effect of 9 kind of ginsenosides on cultured spinal neurons from embryonic rat. *Journal of Brain and Nervous Diseases* **8**: 331–333. https://doi.org/10.3969/j.issn.1006-351X.2000.06.004

Pei L, Meng S, Yu W, Wang Q, Song F, Ma L (2016). Inhibition of MicroRNA-383 ameliorates injury after focal cerebral ischemia via targeting PPARγ. *Cellular Physiology and Biochemistry* **39**: 1339–1346. https://doi.org/10.1159/000447838

Peng T, Liu YH, Chen SH (2008). Effect of ginsenoside Rg1 on the survival rate and neuronal plasticity of primary cultured cortical neurons. *West China Medical Journal.*

Petrescu GED, Sabo AA, Torsin LI, Calin GA, Dragomir MP (2019). MicroRNA based theranostics for brain cancer: Basic principles. *Journal of Experimental & Clinical Cancer Research* **38**: 231. https://doi.org/10.1186/s13046-019-1180-5

Rong W, Xiong J, Wu XT, Yang L, Zhang J, Yan Y (2020). Protective effect of ginsenoside Rg1 on ischemic stroke rats and its mechanism. *Chinese Journal of Clinical Pharmacology* **36**: 4.

Schnegg CI, Robbins ME (2011). Neuroprotective mechanisms of PPARδ: Modulation of oxidative stress and inflammatory processes. *PPAR Research* **2011**: 373560. https://doi.org/10.1155/2011/373560

Sepramaniam S, Tan JR, Tan KS, DeSilva DA, Tavintharan S et al. (2014). Circulating microRNAs as biomarkers of acute stroke. *International Journal of Molecular Sciences* **15**: 1418–1432. https://doi.org/10.3390/ijms15011418

Shi ZY, Zeng JZ, Wong AST (2019). Chemical structures and pharmacological profiles of ginseng saponins. *Molecules* **24**: 2443. https://doi.org/10.3390/molecules24132443

Singh A, Sen D (2017). MicroRNAs in Parkinson's disease. *Experimental Brain Research* **235**: 2359–2374. https://doi.org/10.1007/s00221-017-4989-1

Tyagi S, Gupta P, Saini AS, Kaushal C, Sharma S (2011). The peroxisome proliferator-activated receptor: A family of nuclear receptors role in various diseases. *Journal of Advanced Pharmaceutical Technology & Research* **2**: 236–240. https://doi.org/10.4103/2231-4040.90879

Villapol S (2018). Roles of peroxisome proliferator-activated receptor gamma on brain and peripheral inflammation. *Cellular and Molecular Neurobiology* **38**: 121–132. https://doi.org/10.1007/s10571-017-0554-5

Wang Y, Hao Y, Lou JL, Ma H, Qiu QY (2004). Effect of ginsenoside Rgl and Rhl on the anti-tumor activity of dendritic cell. *Chinese Journal of Pathophysiology* **20**: 1759–1763.

Wang C, Li YZ, Wang XR, Lv ZR, Shi DZ, Liu XH (2012a). Panax quinquefolium saponin attenuates hypoxia/reoxygenation injury in rat cardiomyocytes by inhibiting excessive endoplasmic reticulum stress. *Chinese Journal of Pathophysiology* **28**: 22–28.

Wang J, Song Y, Zhang Y, Xiao H, Sun Q et al. (2012b). Cardiomyocyte overexpression of miR-27b induces cardiac hypertrophy and dysfunction in mice. *Cell Research* **22**: 516–527. https://doi.org/10.1038/cr.2011.132

Wang L, Wang YP, Xu SQ, Sun CH, Yan S, Liu JY, Wang YY, Hou W, Yin P (2007). A review on studies of the components and pharmacological activity of Panax quinquefolium L. *Special Wild Economic Animal and Plant Research* **3**: 73–77.

Wang CL, Yin HJ, Shi DZ, Liu JG (2006). Review on cardiovascular pharmacology of Panax Quinquefolium saponins. *Traditional Chinese Drug Research and Clinical Pharmacology* **1**: 76–78.

Wu L, Xiong X, Wu X, Ye Y, Jian Z, Zhi Z, Gu L (2020). Targeting oxidative stress and inflammation to prevent ischemia-reperfusion injury. *Frontiers in Molecular Neuroscience* **13**: 28. https://doi.org/10.3389/fnmol.2020.00028

Yang Y, Li X, Zhang L, Liu L, Jing G, Cai H (2015). Ginsenoside Rg1 suppressed inflammation and neuron apoptosis by activating PPARγ/HO-1 in hippocampus in rat model of cerebral ischemia-reperfusion injury. *International Journal of Clinical and Experimental Pathology* **8**: 2484–2494.

Zeng Y, Xie K, Dong H, Zhang H, Wang F, Li Y, Xiong L (2012). Hyperbaric oxygen preconditioning protects cortical neurons against oxygen-glucose deprivation injury: Role of peroxisome proliferator-activated receptor-gamma. *Brain Research* **1452**: 140–150. https://doi.org/10.1016/j.brainres.2012.02.063

Zhai FG, Guan LX, Bao HH, Guo SF (2011). Effect of Panax quinquefolium saponins from stems and leaves on acidosis and the metabolism of free radical in focal cerebral ischemia injury rats. *Chinese Journal of Primary Medicine and Pharmacy* **18**: 4–6.

Zhai F, Zhang X, Guan Y, Yang X, Li Y, Song G, Guan L (2012). Expression profiles of microRNAs after focal cerebral ischemia/reperfusion injury in rats. *Neural Regeneration Research* **7**: 917–923. https://doi.org/10.3969/j.issn.1673-5374.2012.12.007

Zhang MX, Fang F, Yang Y, Fan JL, Yuan P (2021). Protective effect of ginsenoside Rg1 on hypoxic-ischemic brain damage and neuronal cell apoptosis in young rats. *Journal of Xi'an Jiaotong University* **42**: 693–699. https://doi.org/10.7652/jdyxb202105009

Zhang XP, Zhai FG, Guan Y, Song GC, Guan L (2012). Changes of microRNA expression profiling in rat cerebral cortex during cerebral ischemia-reperfusion injury. *Chinese Journal of Cerebrovascular Diseases* **10**: 1799–1808. https://doi.org/10.4103/1673-5374.170302

Zhou Y, Li HQ, Lu L, Fu DL, Liu AJ, Li JH, Zheng GQ (2014). Ginsenoside Rg1 provides neuroprotection against blood brain barrier disruption and neurological injury in a rat model of cerebral ischemia/reperfusion through downregulation of aquaporin 4 expression. *Phytomedicine: International Journal of Phytotherapy and Phytopharmacology* **21**: 998–1003. https://doi.org/10.1016/j.phymed.2013.12.005